HEFAT2007
5th International Conference on Heat Transfer, Fluid Mechanics and Thermodynamics
Sun City, South Africa
Paper number: LA1

EXPERIMENTAL AND NUMERICAL STUDY OF BUBBLE-PUMP PERFORMANCE OPERATED WITH A BINARY ORGANIC MIXTURE

Levy A.
Pearlstone Centre for Aeronautical Engineering Studies
Mechanical Engineering Department,
Ben-Gurion University of the Negev,
P.O. Box 653, Beer-Sheva 84105,
Israel,
E-mail: avi@bgu.ac.il

ABSTRACT

A two-fluid model was used to model and simulate the flow of an organic binary mixture through a generator and a bubble pump tube. Both thermal and non-thermal equilibrium conditions were examined. Results obtained from a steady state steady flow experimental system operated with R22-DMAC (chlorodifuoromethane- N-N' dime-thylacetamide) as working fluids were used to validate the predictions of the numerical simulations. The predictions of the numerical simulations for various heat sources on the flow characteristics were compared with the experimental results. Based on the numerical simulations detailed description of the flow characteristics inside the generator and the bubble pump tube were obtained.

INTRODUCTION

The bubble pump is the motive force of the diffusion absorption cycle and is a critical component of the absorption diffusion refrigeration unit. The purpose of the bubble pump (besides the circulation of the working fluid) is to desorb the solute refrigerant from the solution. Therefore the efficiency of the bubble pump is set by the amount of the refrigerant desorbed from the solution. The performance of the diffusion absorption cycle depends primarily on the efficiency of the bubble pump. For that reason it was decided to investigate both numerically and experimentally the performance of the bubble pump for a new diffusion absorption cycle operated with R22-DMAC.

When a fluid flows vertically up in a tube, which is heated either uniformly along the entire tube length or just at the first tube section, the flow pattern of the two-phase flow is continuously changing along the heating section of the tube due to mass transfer. The evaporation of the volatile phase causes a continuous change of both the liquid and the gas flow rates. Typical flow patterns, tube wall and fluid temperatures and the heat transfer ranges in a vertical flow heated tube are presented in Stephan [1] and Collier and Thome [2]. Numerical simulation of two phase flows with heat and mass transfer raises many different and difficult issues, from both modelling and computational points of view. Various theoretical approaches based on mass, momentum and energy balances can be adopted. While considering the phases' interactions and modes of flows, which can be found in evaporation, condensation, absorption and desalination, the two-fluid model seems to be the most suitable approach for describing this process. Therefore many researchers adopted the two-fluid model for modelling similar processes, e.g. [3-8].

NOMENCLATURE

f_{L0}	[kJ/kg K]	Friction coefficient
h	[kJ/kg K]	Enthalpy
$\dot{m}$	[m^{3}K/W]	Volumetric mass transfer rate
$\dot{q}$	[W/m^3]	Volumetric heat generation density
q	[W/m^3]	Volumetric heat transfer
F	[N/m^3]	Force per unit volume
Re	[K]	Reynolds number
T	[K]	Temperature
P	[Pa]	Pressure
u	[m/s]	Velocity
z	[m]	Cartesian axis direction

Special characters

φ	[-]	Gas volume fraction
ρ	[kg/m^3]	density
ξ	[-]	Mass fraction of the refrigerant in the solution

Subscripts

l	Liquid phase
i	Phases interface
WL	Wall
rl	Refrigerant in the liquid phase
a	Absorbent
mix	Access property
g	Gas phase
gl	Transfer property between the phases

Superscripts

*	Equilibrium condition

Levy et al. [8] investigated the convective boiling of binary organic solution in vertical tube. Based on the simplified assumptions (One-dimensional flow; Steady state flow; Constant heat flux at the generator; Constant tube diameter (i.e., cross-section area); Uniform cross-section fluids properties; Compressible gas and liquid phases; Thermal equilibrium (i.e., both phases are at the same temperature); Absorbent vapour in the gas phase can be neglected; Friction force between the vapour phase and the wall per unit volume can be neglected) balance equations for the single- and the two-phase flows were developed. The developed model was used to simulate the convective boiling of binary organic solution in vertical tube.

Koyfman et al. [9] investigated experimentally the performance of the bubble pump for diffusion absorption refrigeration units. A continuous experimental system was designed, built and operated. An experimental parametric study was conducted to examine the influence of parameters such as heat input, motive head, operating pressure and tube diameter on the bubble pump performance. Based on a system analysis it was concluded that the poor solution can be regards as in equilibrium at the bubble pump outlet although it is not at equilibrium condition at the generator outlet. For this reason, the assumption of thermal equilibrium (i.e., both phases are at the same temperature) that made by Levy et al. [8] is not justified all the way through the generator and convective tube.

In the present study experimental and numerical study of bubble-pump performance operated with a binary organic mixture was conducted. The solution was composed of organic solvent and hydrofluorocarbon refrigerant, dimethylacetamide (DMAC) and chlorodifluorometane (R22), respectively. The two-fluid model was used to model and simulates the flow characteristics along the bubble-pump tube and the heating section. In contrary to Levy et al. [8] model, non-thermal equilibrium assumption was made. The model was used for further system analysis and obtaining some design parameters for the bubble-pump tube and the heating section. A continuous experimental system was used to investigated the bubble-pump performance and to validate the model's predictions.

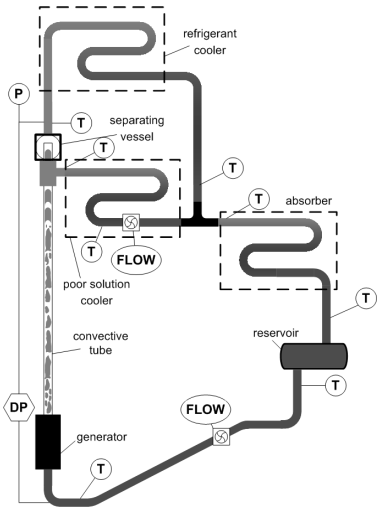

Figure 1 Schematic illustration of the experimental system.

Table 1: Experimental times averaged flow properties as obtained experimentally for various heat inputs and driving head 0.62 m..

	Heat Input [Watt]	**140**	**160**	**180**	**200**	**220**	**240**
Temp. [°C]	Gen. In	27.97	29.55	30.41	28.68	29.45	30.09
	Ref. H.E. in	29.98	32.82	33.84	34.48	37.42	40.61
	Ref. H.E. out	25.47	26.44	26.84	25.71	26.87	28.05
	P.S. H.E. in	44.33	47.78	49.57	49.23	52.87	58.37
	P.S. H.E. out	35.70	40.71	42.07	41.25	43.77	45.77
	Absorber in	38.81	42.51	44.20	43.90	46.72	49.11
	Absorber out	35.83	38.24	39.47	38.57	40.95	42.63
	Reservoir out	35.63	38.30	39.54	38.53	40.70	42.04
[10^{-5} Pa]	Sys. Pressure	3.584	3.881	4.036	3.970	4.259	4.485
[10^{-2} Pa]	Pressure diff.	51.064	50.159	49.855	49.423	49.192	50.159
[ml/min]	Rich Sol. flow rate	90.90	97.32	100.50	104.46	104.58	96.00
[ml/min]	Poor Sol. flow rate	75.72	83.58	85.74	88.62	87.96	77.28

EXPERIMENTAL SETUP AND RESULTS

Schematic illustration of the experimental system is presented in Fig. 1. Rich solution is pumping out from the reservoir, cooled down and flows through a flow meter to a generator unit where the solution gains heat. The desorption process at the generator creates small vapour bubbles which merge into larger bubbles. The rising bubbles form slugs that occupy the whole cross section of the glass tube and flow with the poor solution to the separating vessel. From the separating vessel, the gaseous phase flows up to the gas heat exchanger and the poor solution flows to the solution heat exchanger. Due to the large difference of the normal boiling temperature between the absorbent and the refrigerant (>200^{o}C), the presence of absorbent vapour in the gas phase may be neglected. The cooled (not condensed) refrigerant vapour and the poor solution enter the absorber and the absorption process takes place. The rich solution from the absorber flows back into the reservoir.

The heating unit, (generator) and the convective glass tube inside diameters were 7 mm. 3/8" copper tubes were bended into oval spirals and used as the absorber, poor solution and refrigerant heat exchangers. T type (copper-constantan) thermocouples, with uncertainty of $\pm 0.3°C$, were mounted along the experimental system. A STS pressure transducer, (ATM model - measuring range of 0-20 bar, $\pm 0.1\% FS$), was used to measure the absolute system. The volumetric flow rates of the poor and the rich solutions were measured by Kobold Pelton turbine flow meters, LM model, measuring range 0.02-1.3 ml/min, with uncertainty of $\pm 0.5\% FS$. The pressure drop across the convective tube and the generator was measured with a Smar differential pressure transducer, LD 301 model, calibrated to 0-200 mbar range, with uncertainty of $\pm 0.075\% FS$. Power is supplied to three 220V/100W electric heaters by a variable transformer 0-220V and measured by a digital wattmeter, with uncertainty of $\pm 1W$. The sensors were connected to a personal computer using a National Instruments DAQPad-4350 data logging system. Data logging application was written using National Instruments LabVIEW. The system

operated continuously until a steady state was obtained. Times averaged of the recorded properties as obtained for various heat input are presented in Table 1.

THE HYDRODYNAMIC MODEL

As describe in the previous section, sub-cooled solution is inserting into the generator, which located at the bottom of the bubble-pump tube. Therefore the model should account both the single- and two-phase flows. Mass, momentum and energy balance equations were written for both flows. The conservation equations for the flow of solution with constant refrigerant concentration were solved for the single-phase flow. Heat supplied to the solution until it reached an equilibrium conditions, i.e., the equilibrium concentration of the refrigerant at the solution pressure and temperature is equal to that of the sub-cooled solution. When equilibrium achieved, refrigerant starts to dissolve from the solution due to additional heat supply and pressure reduction; the concentration of the refrigerant in the solution decreases; two-phase flow is initiated while the volume fraction of the gas phase increases. Generally, the gas phase is composed of both absorbent and refrigerant vapours. However, due to the large difference of the normal boiling temperature between the absorbent and the refrigerant, the existence of absorbent vapour in the gas phase may be neglected, as was assumed in this study.

The developed model is based on the following assumptions: One-dimensional flow; Steady state flow; Constant heat flux at the generator; Constant tube diameter, i.e., cross-section area; Uniform cross-section fluids properties; Compressible gas and liquid phases; Absorbent vapour in the gas phase can be neglected; Friction force between the gas phase and the wall per unit volume can be neglected. Finally thermal and non-thermal equilibrium conditions between the phases were examined (i.e., both phases having the same temperature or different temperatures, respectively).

Based on these simplified assumptions balance equations for the single- and the two-phase flows were written.

Single-Phase Flow Governing Equations $\left(\xi^* > \xi\right)$

Solution mass, momentum and energy balances

$$\frac{\partial}{\partial z}\left(\rho_l u_l\right) = 0 \tag{1}$$

$$\frac{\partial}{\partial z}\left(\rho_l {u_l}^2\right) + \frac{\partial P}{\partial z} = -F_{WL} \tag{2}$$

$$\frac{\partial}{\partial z}\left(\rho_l u_l\left(h_l + \frac{u_l^2}{2}\right)\right) = \dot{q} \tag{3}$$

The solution's enthalpy, $h_l \left(\equiv \xi h_{rl} + \left(1-\xi\right)h_a + \triangle h_{mix}\right)$, was calculated as a function of the composition, the enthalpy of the refrigerant in the liquid phase, $h_{rl} = f\left(T\right)$, the enthalpy of the absorbent, $h_a = f\left(T\right)$ and solution's excess enthalpy, $\triangle h_{mix} = f\left(T,\xi\right)$ [10]; The solution density was calculated as function of the composition, refrigerant and absorbent densities [11]. The single-phase balance equations were solved numerically. The refrigerant concentration kept constant and when it reached the value of the equilibrium concentration, $\xi^* = f\left(T,P\right)$, the single-phase flow solver stopped and the two-phases flow solver was initiated.

Two-Phase Flow Governing Equations

Total, vapour phase and refrigerant mass balances

$$\frac{\partial}{\partial z}\left(\left(1-\varphi\right)\rho_l u_l + \varphi\rho_g u_g\right) = 0 \tag{4}$$

$$\frac{\partial}{\partial z}\left(\varphi\rho_g u_g\right) = \dot{m} \tag{5}$$

$$\frac{\partial}{\partial z}\left(\left(1-\varphi\right)\xi\rho_l u_l + \varphi\rho_g u_g\right) = 0 \tag{6}$$

Vapour phase and total momentum balances

$$\frac{\partial}{\partial z}\left(\varphi\rho_g {u_g}^2\right) + \varphi\frac{\partial P}{\partial z} = \dot{m}u_i - F_{gl} \tag{7}$$

$$\frac{\partial}{\partial z}\left(\varphi\rho_g {u_g}^2\right) + \frac{\partial}{\partial z}\left(\left(1-\varphi\right)\rho_l u_l u_l\right) + \frac{\partial P}{\partial z} = -F_{WL} \tag{8}$$

Total energy balance

$$\frac{\partial}{\partial z}\left(\varphi\rho_g u_g\left(h_g + \frac{u_g^2}{2}\right)\right) + \frac{\partial}{\partial z}\left(\left(1-\varphi\right)\rho_l u_l\left(h_l + \frac{u_l^2}{2}\right)\right) = \dot{q} \tag{9}$$

As mentioned above, in the present study both thermal and non-thermal equilibrium conditions were examined. When thermal equilibrium condition was examined it was assumed that both phases have the same temperature and therefore only the total energy balance equation was used. However for the non-thermal equilibrium condition (i.e. both phases have different temperatures), the gas phase energy balance equation was added.

$$\frac{\partial}{\partial z}\left(\varphi\rho_g u_g h_g\right) = \dot{m}h_i + q_{gl} \tag{10}$$

The vapour phase enthalpy was taken as the enthalpy of the refrigerant as function of pressure and temperature. Three additional models for calculating the wall and vapour-liquid friction forces and the heat transfer between the phases (for non-thermal equilibrium condition) were introduced in order to solve the complete model. The additional models that adopted here were used and recommended by Richter [3] & Yang and Zhang [7]. The liquid wall friction force introduce from Martinelli & Nelson [12].

$$F_{WL} = f_{Lo}\left(\frac{1-x}{1-\varphi}\right)^{1.75}\frac{\left(\varphi\rho_g u_g + (1-\varphi)\rho_l u_l\right)^2}{2\left(\varphi\rho_g + (1-\varphi)\rho_l\right)D_{pipe}} \qquad (11)$$

$$f_{Lo} = \left(0.79\ell n\,\mathrm{Re}_{Lo} - 1.64\right)^{-2}$$

The interfacial force between the phase, F_{gl}, for bubble $(\varphi < 0.3)$ and annular $(\varphi > 0.8)$ flow regimes assumed to be known (For more details see [3], [7] and [8]).

$$F_{gl} = \frac{3}{4}\frac{C_d^*}{d}\varphi(1-\varphi)^3\rho_l\left(u_g - u_l\right)\left|u_g - u_l\right| \quad (\varphi < 0.3)$$

$$F_{gl} = 3\frac{C_d}{D_{pipe}}\sqrt{\varphi}\rho_g\left(u_g - u_l\right)\left|u_g - u_l\right| \qquad (\varphi > 0.8) \quad (12)$$

The drag coefficient for bubbly flow, $C_d^* = C_d(1-\varphi)^{-4.7}$, reflects the influence of the bubbles on each other and therefore depends on the gas phase volume fraction [13].

$$C_d = \begin{cases} \frac{24}{\mathrm{Re}_d}\left(1 + 0.15\,\mathrm{Re}_d^{0.687}\right) & \mathrm{Re}_d \le 1000 \\ 0.44 & \mathrm{Re}_d > 1000 \end{cases} \qquad (\varphi < 0.3)$$

$$C_d = 0.005\left(1 + 75(1-\varphi)\right) \qquad (\varphi > 0.8) \quad (13)$$

The momentum balances of both phases are valid for all flow regimes that might be observed in the bubble pump tube, however the interfacial forces that are known are restricted to bubbly and annular flow regimes, where the gas volume fraction is below 0.3 or above 0.8, respectively. In the present study it was assumed that the drag force in between bubbly and annular flow regimes (i.e., in the intermediate flow regimes: plug flow, churn flow and wispy-annular flow) can be linearly interpolated with respect to the gas phase volume fraction. Similar assumption was used for calculating the heat transfer coefficient between the phases when non-thermal equilibrium conditions were examined.

The numerical solution of the above balance equations was obtained using Gear's fifth order BDF method, which is available in the IMSL library. The simulation starts at ahead of the boiling chamber and stopped at the end of the bubble pump tube (i.e., separation vessel).

MODELS VALIDATION AND COMPARISON

The models were solved numerically for simulating the experiments with various heat inputs, rich solution mass flow rate and operating pressure, in which their times averaged properties are presented in Table 1. The following inlet conditions were specified: solution's temperature, operating pressure, concentration and volumetric flow rate. The inlet concentration was calculated, based on vapour liquid equilibrium (VLE) assumption at the reservoir, as a function of the reservoir temperature and the system pressure. The solution inlet velocity was calculated from the volumetric flow rate. In the transition between the single- and the two-phase models,

Table 2: Models compressions with experimental data.

	Heat Input [Watt]	**140**	**160**	**180**	**200**	**220**	**240**
Poor Solution Temp. [°C]	Experimental SD%	0.03%	0.05%	0.05%	0.06%	0.05%	0.09%
	Prediction of TEM	52.08	56.03	59.50	59.96	64.80	72.98
	TEM Error	-2.44%	-2.57%	-3.08%	-3.33%	-3.66%	-4.41%
	Prediction of NTEM	52.08	56.03	59.50	59.96	64.80	72.98
	NTEM Error	-2.44%	-2.57%	-3.08%	-3.33%	-3.66%	-4.41%
Poor solution volume flow rate [ml/min]	Experimental SD%	1.17%	1.33%	2.83%	2.87%	1.24%	6.25%
	Prediction of TEM	78.09	82.93	84.32	86.56	85.22	75.05
	TEM Error	-3.13%	0.77%	1.66%	2.33%	3.11%	2.88%
	Prediction of NTEM	78.09	82.93	84.32	86.56	85.22	75.05
	NTEM Error	-3.13%	0.77%	1.66%	2.33%	3.11%	2.88%
Pressure drop [10^2 Pa]	Experimental SD%	2.13%	1.97%	2.18%	2.78%	3.02%	4.11%
	Prediction of TEM	50.98	50.94	50.18	49.72	49.13	49.64
	TEM Error	0.16%	-1.56%	-0.65%	-0.60%	0.13%	1.04%
	Prediction of NTEM	50.98	50.94	50.18	49.72	49.13	49.64
	NTEM Error	0.16%	-1.56%	-0.65%	-0.60%	0.13%	1.04%

continuous liquid properties were used, and a very small gas mass flow rate per unit area was assumed (10^{-8} kg/m^2). To conserve the total mass balance, the mass flow rate of the gas phase was subtracted from that of the liquid phase and then the gas volume fraction was calculated. By integrating the balance equations along the convective tube, the outlet conditions of the flow at the separation vessel were predicted.

Three additional assumptions have been made in order to validate the numerical simulations predictions. The first, the poor solution temperature at the separation vessel is similar to the one measured at the poor solution heat exchanger inlet (see Fig. 1). The second, the pressure drop across the separation vessel is negligibly small and therefore the predicted pressure drop is equal to the measured one. The third, the predicted volume flow rate of the poor solution is equal to the measured solution's volume flow rate at the outlet of the poor solution heat exchanger. This assumption can be justified by an efficient separation process, i.e., the separated gas can not flow into the solution heat exchanger due to a liquid trap. Based on these assumptions the predictions of the simulations could compare with the experimental data. Table 2 present comparisons between the predictions of the Thermal Equilibrium Model (TEM) and the Non-Thermal Equilibrium Model (NTEM) and the experimental data for the poor solution temperature, volume flow rate and the pressure drop. An error is defined by

$$Error\ [\%] = \frac{\text{Experimental Value - Predicted Value}}{\text{Experimental Value}} \qquad (14)$$

The validity of the TEM and the NTEM and their assumptions can be clearly seen in Table 2. The predicted pressure drops along the generator and the bubble pump tube varied between 1.1% to -1.6% from the experimental values. As can also be seen, the deviations of the predicted pressure drops from the experimental values are less that the experimental standard deviation values. The predicted poor solution flow rates varied between 3.2% to -3.2% from the experimental values, while the experimental standard deviations were up to 6.25%. Both models over predicted the poor solution temperature at the bubble pump outlet by up to 4.5%. This might be due to the assumption that the poor

solution temperature at the separation vessel is similar to that measured at the poor solution heat exchanger inlet. Therefore, the difference between the predicted values at the bubble pump outlet and the measured at the poor solution heat exchanger inlet can be justified by heat loses.

The predictions of the TEM and the NTEM show similar values at the bubble pump outlet. This results form the equilibrium conditions achieved in the bubble pump tube. Figure 2 presents comparison between the predictions of the TEM (black lines) and the NREM (blue lines) for the gas volume fraction, solution concentration, phases' velocities and temperatures and pressure along the heating section and the part of the bubble pump tube as obtained by the numerical simulations for 180W generator (see Table 1). The four vertical dashed lines represent locations within the heating section. The first and the last mark the location of the heating section while the second and the third mark the transition from sub-cooled flow to bubble flow and then to plug, churn or wispy-annular flow regimes, respectively.

As can be seen in Figure 2, sub-cooled solution is enter the vertical tube, the pressure is being drop due to gravity and wall friction until it enters to the heating section. The solution is being heat rapidly until the solution reached the equilibrium temperature. At this point (second vertical line), further heating results in gas generation by desorbing of refrigerate from the solution. Bubbles are formed and due to densities difference (gravity), their velocity increases rapidly towards their terminal velocity. Due to the increase in the average diameter of the bubbles and the increase of gas volume fraction, the velocity of the bubbles then starts to decrease (Fig. 2b). The refrigerant desorption from the solution causes a decrease in the rate of temperature and pressure changes. The gas phase is accelerating and drags the liquid upwards. Additional gas is being separated from the solution due to both pressure reduction (flashing) and temperature increases (heat supplied).

When the two-phase flow leaves the heating section, the pressure is continuously dropped due to friction and gravity. This results in minor changes in phases' velocities and temperature. In the TEM, the small reduction of the pressure cause to a minor decrease in both the liquid and the gas temperatures. In the NTEM, the gas phase temperature increases due to heat exchange with the liquid phase, until it reaches thermal equilibrium condition. From that point onward a minor decrease in both the liquid and the gas temperatures may be observed due to the small pressure reduction while the solution concentration and gas volume fraction practically remains constant.

The main difference between the TEM and the NTEM can be seen in Figure 2c. In the NTEM, the gas phase temperature (the dashed blue line) is lower than the equilibrium temperature. However, due to high heat and mass transfer between the phases in the bubbly flow regime, this temperature difference is negligible. Except from the lower gas phase temperature at the generator outlet, there is no much difference between the models. Therefore the TEM model, in which used less semi-empirical models for calculating the heat transfer between the phases might be preferable for further analysis and system design.

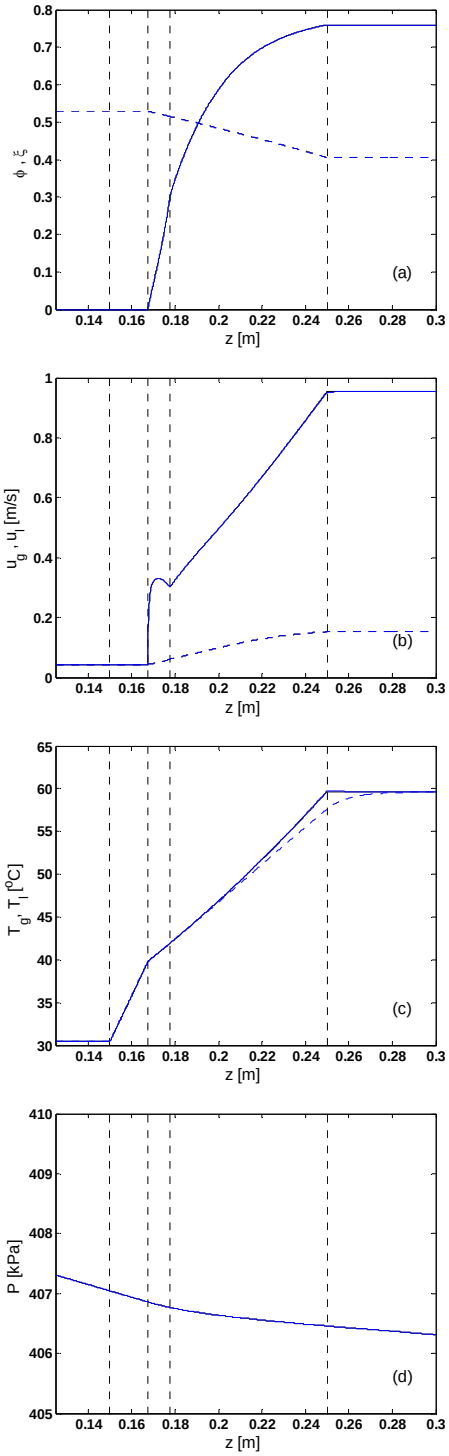

Figure 2 Comparison between the predictions of the TEM (black lines) and the NTEM (blue lines) as obtained for 180Watt heat input. (a) gas volume fraction (solid line) & solution concentration (dashed line), (b) gas and liquid phases' velocities (solid & dashed lines, respectively), (c) liquid and gas phases' temperatures (solid & dashed lines, respectively) and (d) pressure along the vertical tube.

THE INFLUENCE OF THE HEAT INPUT

The influence of the heat input to the generator on the bubble pump performance was investigated. It was obtained that for constant driving head increasing the heat input results in higher rich and poor solutions flow rates, higher outlet temperature and lower pressure drop across the bubble pump and the bubble pump tube. The reduction of the pressure drop resulted from the higher refrigerant volume fraction in the bubble pump tube for higher heat input. It should be noted that although the poor solution flow rate increases, more refrigerant dissolved from the solution for higher heat input. Therefore the pumping ratio (defined as the ratio between the poor solution and the refrigerant mass flow rates) decreases as the heat input increases. The influence of the driving head on the bubble pump performances was also investigated. It was obtained that increasing the driving head increases both the pressure drop and the poor solution flow rate.

THE INFLUENCE OF THE OPERATING PRESSURE

The influence of the operating pressure on the flow characteristics was examined numerically. The predictions were obtained for the inlet conditions specified in Table 1 with 200W input and various operating pressures. These predictions could not be validated since in a closed continuous system, such as ours, the operating pressure and inlet temperature cannot be controlled for a given heat input. Since the rich solution in the reservoir (see Fig. 1) is in equilibrium condition, higher refrigerant concentration obtained when the operating pressure is higher. For the same heat input, more refrigerant desorbed from the solution, when solution with higher refrigerant concentration flow through the generator and the bubble pump tube. Nevertheless, the gas volume fraction was decreased. This resulted from the hydrodynamic model which considered compressible gas and liquid phases. Denser gas and liquid phases result in lower phases' velocities. The influence of the operating pressure on the solution temperature and pressure drop was negligibly small.

CONCLUSION

Numerical and experimental study of bubble pump performance was conducted. A continuous experimental system was operated to validate the predictions of the numerical simulations. A two-fluid model was used to model flows in both thermal and non-thermal equilibrium conditions. The models were solved numerically to simulate the flow and to obtain the characteristic flow profiles along the generator and the bubble pump tube. The predictions of the numerical simulations were validated experimentally.

The assumption that due to the large difference between the normal boiling temperature of the absorbent and that of the refrigerant (more than 200°C), the presence of absorbent vapour in the gas phase could be neglected was justified by the good agreement between the predictions of both models and the experimental data. However, this assumption limiting the models to simulating flow boiling of binary mixtures for which there is a large difference of normal boiling temperature between absorbent and refrigerant.

On the basis of the numerical simulations, a detailed description of the flow characteristics inside the generator and the bubble pump tube was obtained. The influence of the heat source and driving head on the flow characteristics was examined both numerically and experimentally.

The comparison between the TEM and the NTEM shows that there is no much difference between them if one looks at the overall performances of the unit. The NTEM relays on more semi-empirical correlations and assumption for calculating the heat transfer between the phases. The inaccuracies of these correlations and additional models may lead to larger discrepancy between the prediction of the numerical simulations and the experimental data. Nevertheless the overall energy balance was conserved, and therefore there was no difference between the predictions of the TEM and the NTEM at the bubble pump outlet. Therefore, for simplicity the TEM should be used for further analysis and system design.

REFERENCES

[1] Stephan, K, Heat Transfer in Condensation and Boiling. Springer-Verlag, Berlin, 1992.

[2] Collier, J. G., Thome, J. R. Convective Boiling and Condensation. 3rd ed., Oxford University Press, Oxford. , 1994.

[3] Richter, H.J. Separated two-phase flow model: application to critical two-phase flow. Int J Multiphase Flow, 1983:9 (5), 511–530.

[4] Prashanth, K.V. and Seetharamu, K.E. FEM predictions for two-phase flow in a vertical pipe without the use of any external correlations. Int. J. Num. Meth. Heat Fluid Flows, 1993:3, 565-575.

[5] Sujatha, K.S., Mani, A., Srinivasa M.S. Finite element Analysis of a Bubble Absorber. Int. J. Num. Meth. Heat Fluid Flow, 1997:7(7), 737-750.

[6] Sujatha, K.S., Mani, A., Srinivasa, M.S. Analysis of a bubble absorber working with R22 and five organic absorbents. Heat and Mass Transfer, 1997:32, 255-259.

[7] Yang, L., Zhang, C.-L. Two-fluid model of refrigerant two-phase flow through short tube orifice. Int. J. Ref., 2005:28(3), 309-458.

[8] Levy, A., Koyfman, A. and Jelinek, M., Flow boiling of organic binary mixtures. International Journal of Multiphase Flow 2006:32, 1300–1310.

[9] Koyfman A., Aharon J., Jelinek M., Levy A. & Borde I., "Experimental investigation of bubble-pump performance operated with R22-DMAC", Submitted for publication.

[10] Borde, I. and Jelinek, M., "Thermodynamic properties of binary fluid mixtures for absorption refrigeration systems", ASME 86-WA/HT-60, 1986.

[11] Jelinek M., Levy A. & Borde I., "Density of Organic Binary Mixtures from Equilibrium Measurements", International Journal of Refrigeration, 2007: 30(3), 471- 481.

[12] Martinelli R. C. and Nelson D. B., Prediction of Pressure Drop during Forced-Circulation Boiling of Water, Trans. ASME, 1948:70(6), 695-702.

[13] Wallis, G. B., 1969, One-Dimensional Two-Phase Flow, McGraw-Hill Book Company, New York.